Vrije Universiteit Brussel

VRIJE
UNIVERSITEIT
BRUSSEL

Optimal Sizing and Aging Investigation of Second Life Lithium-ion Battery Using Renewable Power Smoothing Stationary Application

Kebede, Abraham Alem; Hosen, Md Sazzad; Kalogiannis, Theodoros; Behabtu, Henok Ayele; Jemal, Towfik; Van Mierlo, Joeri; Coosemans, Thierry; Berecibar, Maitane

Citation for published version (APA):
Kebede, A. A., Hosen, M. S., Kalogiannis, T., Behabtu, H. A., Jemal, T., Van Mierlo, J., Coosemans, T., & Berecibar, M. (2022). Optimal Sizing and Aging Investigation of Second Life Lithium-ion Battery Using Renewable Power Smoothing Stationary Application. In *2022 IEEE Vehicle Power and Propulsion Conference, VPPC 2022 - Proceedings* (2022 ed., pp. 1-6). (2022 IEEE Vehicle Power and Propulsion Conference, VPPC 2022 - Proceedings). IEEE. https://doi.org/10.1109/VPPC55846.2022.10003353

Optimal Sizing and Aging Investigation of Second Life Lithium-ion Battery Using Renewable Power Smoothing Stationary Application

Abraham Alem Kebede[1,2]
[1] MOBI research group,
Vrije Universiteit Brussel (VUB),
Belgium
[2] Faculty of Electrical and computer engineering, Jimma University, Jimma, Ethiopia.
abraham.alem.kebede@vub.be /
abrahamece28@gmail.com

Md Sazzad Hossen[1]
[1] MOBI research group,
Vrije Universiteit Brussel (VUB),
Belgium

Theodoros Kalogiannis[1]
[1] MOBI research group,
Vrije Universiteit Brussel (VUB),
Belgium

Henok Ayele Behabtu[1,2]
[1] MOBI research group,
Vrije Universiteit Brussel (VUB),
Belgium
[2] Faculty of Electrical and computer engineering, Jimma University, Jimma, Ethiopia.

Towfik Jemal[2]
[2] Faculty of Electrical and computer engineering, Jimma University, Jimma, Ethiopia

Joeri Van Mierlo[1]
[1] MOBI research group,
Vrije Universiteit Brussel (VUB),
Belgium

Thierry Coosemans[1]
[1] MOBI research group,
Vrije Universiteit Brussel (VUB),
Belgium

Maitane Berecibar[1]
[1] MOBI research group,
Vrije Universiteit Brussel (VUB),
Belgium

Abstract—**Integration of large renewable energy sources (RESs) to the grid is aimed to solve the problem of shortage of power with the production of surplus energy and satisfy the increasing demand. However, the intermittent nature of RESs is challenging to integrate with the grid system. Therefore, the utilization of storage batteries, particularly the re-use of retired electric vehicle batteries for stationary application is therefore a reliable solution to mitigate this problem. In order to evaluate the performance of second life batteries in stationary application, first, the optimal sizing of storage batteries and the cycling profile definitions are performed. Based on the defined cycling current profiles, the second life aging of retired battery cells is conducted at the cell and module level aspects. From the result of the study, it is found that the technical performance of second life batteries is promising and can be regarded as a viable solution for the integration of RESs with the grid system.**

Keywords— Electric vehicle; Renewable energy source; Retired battery; Aging; Stationary application.

I. INTRODUCTION

The technological advancement in lithium-ion (Li-ion) batteries have favored electric vehicles (EVs) to be driven for long distances and mitigate greenhouse gas emissions [1]. Though the technical and environmental contribution of Li-ion battery technologies is found to be promising, the huge capital investment becomes a barrier for its extensive utilization in automotive and different stationary applications [2]-[4]. Nevertheless, when these battery technologies are retired from their EVs service, they retain almost 80 percent of the usable capacity [5]-[7], which can be utilized in other low demanding stationary applications. With the prevalent use of Li-ion battery technologies, various car manufacturers are engaged on the re-use of second life batteries (SLBs) which is expected to reach a potential of more than 26 GWh by 2025 [8].

Therefore, rather than disposing of retired batteries, the re-purposing or re-using of these much amount of SLBs provides a significant advantage interms of techno-economic and environmental aspects [9], [10]. To date, there is no clearly defind demarcations on the performance status and lifetime of the SLBs to be used in relatively high demanding stationary applications while some studies investigated the aging aspects [11], [12].

To perform the technical viability evaluation of SLBs, in this paper, an assessment of suitable second life application is carried out to improve the utilization of retired batteries, increasing their useful life beyond the EVs service life. With this fact, in addition to the technical performance evaluation, the total cost of ownership and therefore, the cost reduction could be possible. To evaluate the technical viability of the SLBs, a methodology is proposed to determine the optimal sizing, and define the cycling aging profile followed by extensive experimental characterization for evaluation of SLBs performance. This methodology includes an optimization process to determine the optimal size of the second life energy storage system according to different objective functions and restrictions. Ones the optimal size is determined the most suitable operation point and the intensity of the cycling pattern is defined based on the real data collected from the existing 10kWp photovoltaic plant installed in Ethiopia [13].

To perform the SLBs aging tests, two types of experimental setup are considered (cell level and module level tests presented in section V). To assess the suitability of SLBs for renewable power smoothing stationary application, cell level aging test is performed with prolonged cycling by taking measurement of state of health (SoH) as function of capacity loss and internal resistance increase parameters. Furthermore,

module level aging test has been performed to evaluate the performance of retired batteries and to evaluate cell to cell heterogeneity effect. The aging characterization methodology followed in this paper is a continuation of the methods used in the previously published paper related with the first life aging study of 43 Ah big capacity battery cell [14]. Meaning the same type of cells has been used for the second life aging investigations performed in this study. In general, the main contribution of the study includes: the optimal sizing of the SLBs, cycling aging profile creation, followed by experimental result findings of aging characterization from first life-beginning of life (FL-BoL) through second life-end of life (SL-EoL). Finally, conclusions are drawn. The rest of the sections are structured as follows: Section II discusses the mathematical optimization and sizing methodology. Section III presents the result of SLBs optimal sizing. Section IV describes the cycling profile definition and pattern development. Section V describes the aging investigation and experimental setup of SLBs. Section VI explain the result and discussion. Section VII presents the conclusions and future work.

II. MATHEMATICAL OPTIMIZATION AND SIZING METHODOLOGY

A. Optimal sizing of second life batteries

The sizing of the selected retired batteries is performed based on the field data collected from the existing photovoltaic grid connected system (PVGCS) which was studied previously [13], where the overall performance analysis and evaluation of the PVGCS system is already presented. The EoL batteries rating and therefore sizing is estimated using real power data collected at the plant for almost one year. For the optimal sizing and smooth operation of the overall system, an efficient algorithm is proposed to determine the accurate sizing of storage battery systems and define the cycling patterns for the respective stationary application profile.

The proposed methodology is based on a Linear optimization programming language using combination of Cplex and Matlab optimization environment. Cplex is an optimization software used to compute optimization of linear and nonlinear functions. The algorithm executes the optimization process using two separate sections, where the first one is the optimal sizing of the storage system, and the second one is determination of the aging profiles and synthesis of cycling patterns used to test the batteries. The flowchart of the proposed methodology for determining the size of the SLBs and the cycling aging profile is shown in Fig. 1.
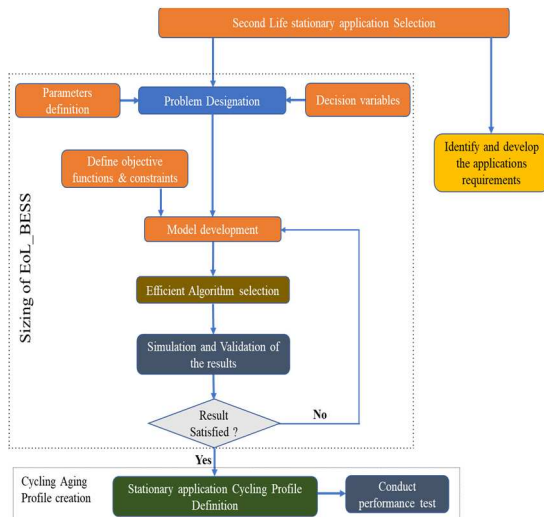

Fig. 1. Summary of the proposed methodology used for sizing and cycling aging profile definition.

From Fig. 1 it can be seen that, during the model development, all the objective functions and constraints are formulated mathematically. Depending on this model, the appropriate optimization algorithm is selected for rating the size of EoL batteries for the selected application. Using the simulation output, the optimization results are validated. After accomplishing the sizing estimation of storage batteries, the cycling profile definition is performed.

The optimal sizing of the SLBs started with the problem identification which consists of input output parameters identification and defining the corresponding decision variables. The main inputs of the power smoothing optimization considered in this study are the PV production profile and the smoothing requirements settled with the RESs integration to the grid. Besides, the respective outputs are PV and the battery storage system generation output, optimal storage size, and the aging result of the SLBs. In this paper, one of the targets is minimization of the storage size by taking in to account the capacity of the SLBs [15] - [17].

B. Optimization process with renewable power smoothing application

The overall optimization process is performed with the definition of objective function and constraints. The design variables of the selected optimization algorithm need also be determined in this step.
The general power balance equation of the existing PVGCS system under study can be given as,

$$P_{PVGCS}(t) = P_{pv}(t) + P_{batt}(t) \qquad (1)$$

Where, P_{PVGCS} is the total power output of the PVGCS at time t, P_{pv} is the output power of the PV plant and P_{batt} is power output of the battery energy storage.

The requirements for the integration of RESs including the PV system are different according to the type of grid code standards to be used. For instance, the ramp rate limit (RRL) requirement for the integration of power plants with the grid system is commonly considered, which was defined by [15]-[17], where the range of 10% per minute compliance is stated as standard [18], [19]. Besides, the design variables related to the SLBs optimization problem are considered which include the nominal battery capacity (Q_{batt}), reference instantaneous capacity (Q_{ref}), instantaneous battery power (P_{batt}), and battery energy (E_{batt}). In the optimization process the design parameters are crucial and therefore minimum promising capacity determination of the battery can be achieved. The battery instantaneous energy and power are used for monitoring the operation mode and status of the SLBs. These parameters are used for computation of the simulation including the PV radiation data which is provided as an input to the model.

C. Daily Optimization process

For the daily optimization problem, the design variables mentioned in section II (B) are used for computation of the optimization process. For simplicity, these design variables composed of the vector "y" of the linear optimization presented. The preparation of mathematical model using Cplex software based linear programming optimization is formulated as shown in Equation (2).

$$\min_{Q_{batt}} Q_{batt} \quad s.t \begin{cases} A.y \le b, \\ A_{eq}.y = b_{eq}, \\ lb \le y \le ub. \end{cases} \qquad (2)$$

Where, Q_{batt} is battery capacity which is the capacity value of the EoL battery system, "y" stands for the solution

vector which represent all constraint variables, "lb" and "ub" represents the lower and upper bound limits of the constraints. The optimization function incorporates the constraints of linear inequalities, linear equations and bounds with the matrix A_{eq} and vector b_{eq} of the optimization problem. The main constraints of the optimization program include, the RRL, the state of charge (SoC) limits, SoH as a function of reference capacity, energy level of the battery, and correlation coefficient value of capacity degradation. The objective function in Equation (2) mainly is subject to the following constraints considering the RRL defined based on the renewable sources grid integration requirement standard. The optimization program is described by the respective in-equalities and equalities, and the expression of the constraint related to the upper and lower bound limit is shown in Equation (3), and Equation (4) respectively.

$$P_{PV}(t) - P_{PV}(t-1) + P_{batt}(t) - P_{batt}(t-1) \leq RRL \quad (3)$$

$$-P_{PV}(t) + P_{PV}(t-1) - P_{batt}(t) + P_{batt}(t-1) \leq RRL \quad (4)$$

In the PVGCS system, the PV plant and the SLBs system is restricted in such a way that the power produced is fed to the grid system. This restriction is given by,

$$P_{PV}(t) - P_{batt}(t) \leq 0 \quad (5)$$

Where, P_{PV} represents the PV plant power output, P_{batt} is the batteries power output and t is the time of the day. The respective operation condition of the battery with in the defined upper and lower SoC limits is given as,

$$-\frac{1}{Freq_{Measured}} P_{batt}(t) + E_{batt}(t) - SoC_{max}.Q_{ref}(t) \leq 0 \quad (6)$$

$$\frac{1}{Freq_{Measured}} P_{batt}(t) - E_{batt}(t) + SoC_{min}.Q_{ref}(t) \leq 0 \quad (7)$$

Where, SoC_{min} (%) and SoC_{max} (%) are the minimum and maximum operating SoC limits respectively. P_{batt} is the power flow and exchange of the SLBs, E_{batt} is the SLBs instantaneous energy in per unit (p.u). Moreover, Q_{ref} is the reference capacity in p.u. at each sample of time. $Freq_{measured}$ is the sampling time in [h^{-1}]. In addition to the above constraints, the operation of the SLBs is restricted in terms of SoH operating limits provided as a function of capacity fade. Therefore, the battery nominal capacity (Q_{batt}) and the instantaneous reference capacity (Q_{ref}) are used for expression of the battery status, and the Q_{ref} should be within the maximum and minimum range of the SoH limits.

$$SoH_{min}.Q_{batt} - Q_{ref}(t) \leq 0 \quad (8)$$

$$-SoH_{SL\_BoL}.Q_{batt} + Q_{ref}(t) \leq 0 \quad (9)$$

Where SoH_{SL_BoL} is the SoH at the second life beginning of life conditions.

The estimation of the capacity fade is given by Equation (10) [18], [19], which is expressed by considering the energy output among two sequential time instants and the degradation coefficient symbolized by K.

$$Q_{ref}(t) - Q_{ref}(t - \Delta t) - K * [E_{batt}(t - \Delta t) - E_{batt}(t)] \leq 0 \quad (10)$$

For the case of the initial or SL-BoL conditions, this equation can be calculated based on the expression shown in Equation (11).

$$-K.[E_{batt}(1) - SoH_{SL\_BoL} * SoC_{SL\_BoL}.Q_{batt}] \leq 0 \quad (11)$$

The required inequalities of the constraints are presented from Equation (3) to Equation (11), which enables to illustrate the optimization problem shown in Equation (2) with the respective matrix A and vector b parameters. In addition to the formulated inequalities, the equality constraints of the SLBs operation equation are presented as follows,

$$E_{batt}(t) - E_{batt}(t - \Delta t) - P_{batt}(t) * \Delta t = 0 \quad (12)$$

By considering the initial SL-BoL conditions, Equation (12), can be rewritten in terms of Equation (13),

$$E_{batt}(1) - SoH_{SL\_BoL} * SoC_{SL\_BoL} * Q_{batt} - P_{batt}(1) * \Delta t = 0 \quad (13)$$

The expressions of Equation (12) and Equation (13) belongs to the equality constraints specified at Equation (2) representing the matrix A_{eq} and vector b_{eq} of the formulated problem optimization. From Equation (12), it can be seen that the change in the instantaneous battery energy equals to the battery power demand during a certain period of time.

D. Global Optimization process

In addition to the optimal sizing of the battery on a daily basis, the global optimal sizing of the SLB is performed using one year operation profile of the PVGCS plant. Recalling similar objective function used on a daily optimization, the design variable of the optimization process for the global optimization is defind, which is the battery rated capacity ($Q_{batt\ global}(t)$) in this case. The objective function intends to find minimum capacity value which satisfies the total year requirement indicated in Equation (14).

$$\min_{Q_{batt}} Q_{batt\ global}(t) \quad (14)$$

The objective function expressed is subjected to different constraints used for optimization of the battery capacity in a yearly basis by considering each day optimization result.

$$\min_{Q_{batt}} Q_{batt\ global} \quad s.t$$

$$\begin{cases} Q_{batt\ global}(t) \geq Q_{batt}(t), \\ Q_{batt\ global}(t) - Q_{batt\ global}(t - \Delta t) = K * total_{dis}(t) \end{cases} \quad (15)$$

From Equation (15) the optimal capacity value for each day of the year ($Q_{batt\ global}(t)$) is equal or greater than the capacity found in prior optimization for each day ($Q_{batt}(t)$). Besides, the degradation of capacity in line with the energy throughput for each respective day is taken into consideration by using the degradation coefficient (K). The constraints considered in Equation (15) can be inclusively expressed with the equality and inequality matrixes and vectors mentioned in Equation (2). These constraints can further be expressed as:

$$-Q_{batt\ global}(t) \leq -Q_{batt}(t) \quad (16)$$

$$Q_{batt\ global}(t) - Q_{batt\ global}(t - \Delta t) = K * total_{dis}(t) \quad (17)$$

Considering the SL-BoL condition, where t is taken as 1 day, Equation (17) can be estimated further in terms of SoH. In addition, accounting one year duration as well the whole expression can be provided as,

$$SoH_{min} * Q_{batt\ global}(1) - Q_{batt\ global}(365) = 0 \quad (18)$$

From Equation (18) it is assumed that the capacity loss of the SLBs throughout the whole year is less than the maximum permitted capacity fade of the SLBs.

III. RESUT OF OPTIMAL SIZING FOR SECOND LIFE BATTERIES

Prior to the utilization of the SLBs for the dedicated stationary application, the ramp rate compliance analysis is performed based on the measurement data from the PV plant. As already mentioned in Section II, the RRL that the plant must be provided is within 10%/minute limit.
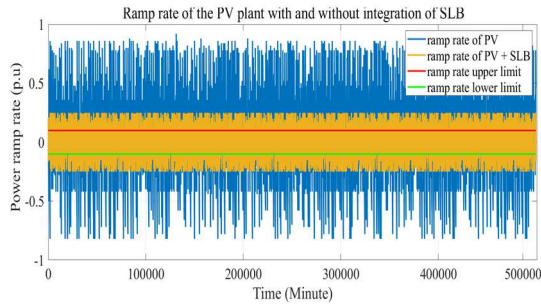
Fig. 2. PV plant and PV plus battery ramp rate analysis of the yearly output power.

Fig. 2 presents the ramp rate result of the PV output before using the SLBs as well as the results when using the smoothing application as a result of the global optimization considering the statistical insight regarding the frequency distribution of different ramp rates over the one-year available data.
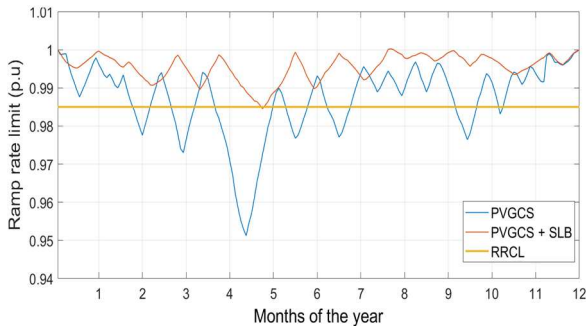

Fig. 3. Ramp rate limit of the PV and PVGCS with SLBs.

Fig. 3 presents the RRL computed for one year operation of the PV plant without SLBs and the other scenario corresponding to the plant operating with the SLBs. The rating of the SLBs is defined by using the proposed optimization technique. From Fig. 3 it can be seen that the RRL are fit with the operating limit while applying the SLB system.

According to the above optimization technique, the optimal value of the SLBs capacity is estimated. These values are plotted in Fig. 4 below showing that there are different values required for the battery capacity depending on the day of the year. For achieving the ramp rate constraints defined in Section II, the SLBs rated capacity is estimated by using the optimal values and energy output profiles. The best possible value of the Q_{ref} is acquired as the lowest value which gives the desired capacity for the SLBs to attain the required power smoothing during the course of the year.
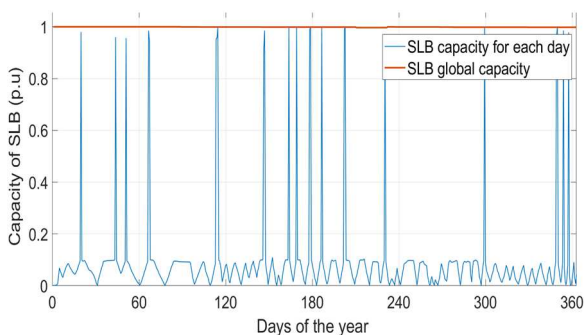

Fig. 4. Capacity rating of the SLB on a daily and global basis.

Fig. 5 shows the energy output of the SLBs during the course of a year, by using the capacity found from the optimization result of the SLBs. The stored energy of the battery is maintained among the boundaries enforced by the energy management of the battery, specified as SOC_{min} (20%) and SOC_{max} (80%).
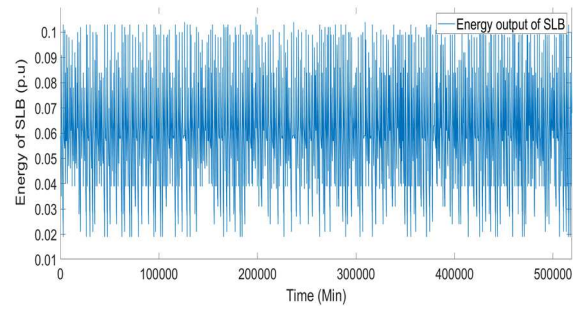

Fig. 5. Annual energy output of the SLB considering renewable power smoothing application.

Fig. 5 shows the SoC upper and lower operation boundaries which reached to the limit repeatedly. Fig. 4 and Fig. 5 together verify that a variable power output of PV with a typical day makes the SLBs to work within 80% to 20% SoC boundaries. Furthermore, several successive and variable energy distribution is found which resulted in an increased demand and enhanced sizing of SLBs. Taking this into account, for the dominant part of the year, the sizing estimation of SLBs is made optimal avoiding the effect of oversizing which in turn is used to monitor the scope of SoC operation range.

IV. PROFILE DEFINITION FOR SECOND LIFE RENEWABLE POWER SMOOTHING STATIONARY APPLICATION

One of the main goals of the study is to achieve accurate cycling profile to be used for SLBs aging test. A real PVGCS is considered as a case study for the evaluation of the results obtained with the presented sizing methodology.

From Fig. 6 it is observed that, the current profile for individual cells of the battery is determined from the total energy required to the SLBs. The resulting current profile in turn is utilized for aging characterization of the SLBs, and this enables to analyse the performance of SLBs and their aging evolution after reaching their end of life. Based on the yearly energy output of the SLBs and the configuration type of the battery pack, the yearly current profile is defined and then the one-month profile is synthesized as shown in Fig. 6.
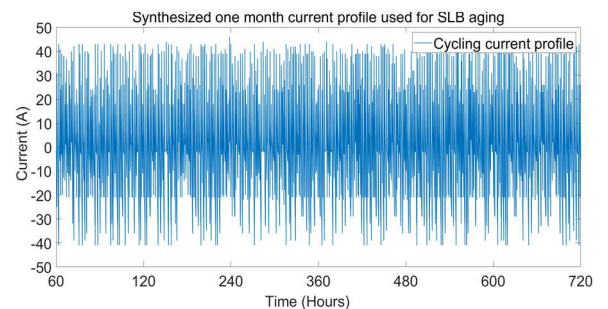

Fig. 6. One-month synthesized current profile used for cycling aging of the SLBs for cell and Module level testing.

V. AGING INVESTIGATION OF SECOND LIFE BATTERIES

A. Experimental setup

This section discussed the procedures used for the collection of experimental data of the SLBs capacity degradation and DC internal resistance tested under cycling aging of stationary application profile. The battery cells used for experimenting is a large format prismatic cell consisted up of NMC/C based cathode and graphite-based anode [20]. Lithium salt or lithium hexafluorophosphate is used as an electrolyte material for these cells and has a nominal capacity of 43 Ah, nominal voltage of 3.6 V, 840 g weight, and high-power density of 1200 W/kg which makes the cell suitable to be used in automotive and stationary application. In addition, the operating voltage region of the cell is 3 to 4.2V with

internal resistance of ≤ 2 mΩ and dimension of 27.5 mm * 148 mm * 91 mm. PEC manufactured testers for testing of the cells and measurement of parameters, and CTS customed climate chambers for ambient temperature control were used. During the lifetime characterization of the SLBs, the performance of the battery cells was tracked through the reference performance tests (RPTs) conducted in line with the cycling aging test. The RPTs include the capacity test, hybrid pulse power characterization (HPPC) test and open circuit voltage (OCV) tests. The overall experimental setup is shown in Fig. 7.
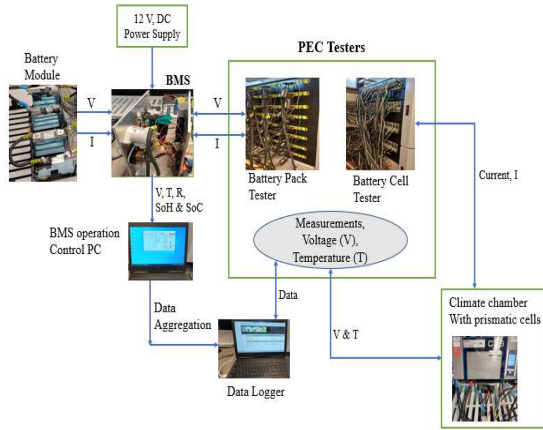

Fig. 7. Experimental setup used for cell level and module level aging test.

B. Schematic representation of the battery cells aging flow

The selected representative battery cells were subjected to second life aging by considering combination of different first life testing conditions and matrixes. As shown from Fig. 8, cells with realistic profiles and cycling aging condition of the first life history was considered to conduct the second life aging of cell level and module level tests. One cell with realistic profile, three cells with cycling aging and one more cell with calendar life (total of five battery cells) was selected for pursuing the second life testing.
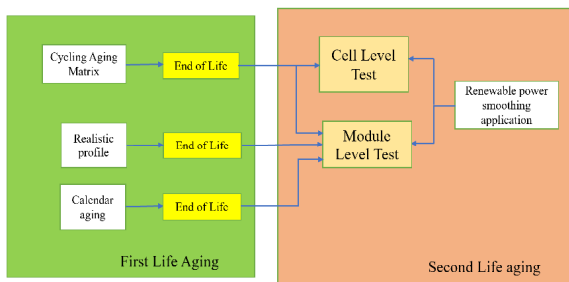

Fig. 8. The flow from first life through second life aging test.

VI. RESULT AND DISCUSSIONS

A. Aging results of second life batteries

Cells tested in their first life with realistic EVs profiles are used for evaluation of EoL batteries performance during stationary application as second life service. The SoH level of the cells at the end of first life is considered as a key factor affecting battery performance and degradation behaviours during second life use.

The test plan and procedure are summarized in Fig. 8, where cells coming from the different first life conditions are distributed and used for cell-level and module level second life testing conditions after being subjected to EoL characterization procedures.

B. Cell level second life aging result

While performing the aging analysis of the battery cells, their capacity loss and internal resistance increase parameters were monitored along with the cell surface temperature, state of charge, current and voltages in both first and second life conditions.
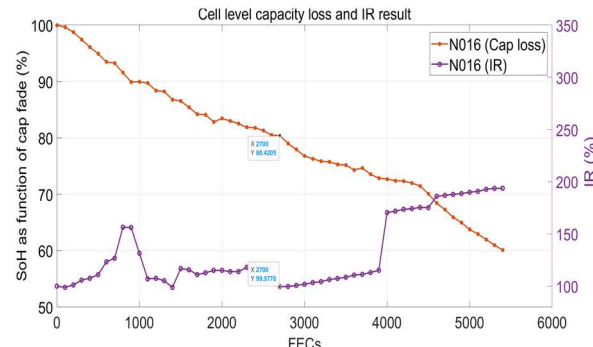

Fig. 9. Cell level capacity loss and resistance increase result from FL-BoL to SL-EoL.

From Fig. 9, it can be seen that the second life battery cell is showing good performance status under second life renewable based stationary application evaluated interms of capacity evolution and internal resistance increase. Moreover, the capacity shows visible capacity loss trends and therefore, the capacity is taken as a promising performance indicator of the SLBs. However, the internal resistance suffers a change of trend almost throughout the lifetime of the SLB cells under study. Unlike the result of the capacity fade, the resistance change is not dominant in terms of aging for these cells. The second life aging test is started at 2700 full equivalent cycles (FECs) with SoH value of 80.42% and DC internal resistance of 99.57%. After 4400 FECs the cell NMC-016 is found to be reached the aging knee where the trend of the capacity degradation is changed. The cell capacity degradation reached to 60.12 % SoH and internal resistance increase of 193.75 % which shows that the cell NMC-016 provides good performance operating for a total of more than 5400 FECs (2700 FECs with EV profile and the other 2700 FECs with stationary renewable power smoothing profile). The battery cell also demonstrates a consistent capacity fade result which shows stable aging performance characteristics.

C. Module level second life battery aging result

Total of four cells was connected in series to form a module level aging analysis. The battery management system (BMS) is utilized to monitor the battery and individual cells' operating parameters while performing the cycling aging test.
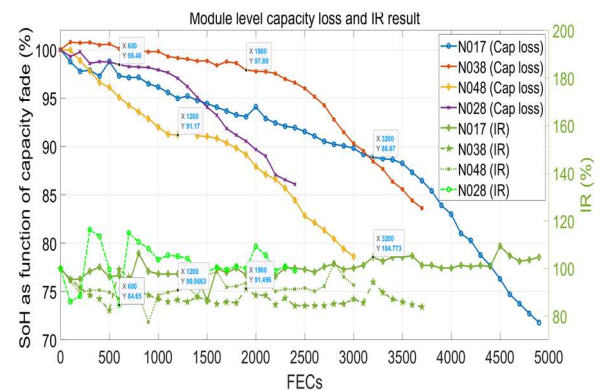

Fig. 10. Module level capacity loss and resistance increase result from FL-BoL to SL-EoL.

Fig. 10 shows that the degradation rate of the cells in the battery module is slightly lower than the cell level degradation rate. This shows that the second life cells aged at an early stage provides lower capacity degradation rate as compared to cell

level capacity fade and therefore better performance is resulted. With the consequences of the first life history, the N017 battery cell which was subjected to aging of realistic profile during its first life, shows observable degradation rate compared to the other cells. It is also shown that at 3600 FECs the cell NMC-017 reaches almost at aging knee where the change of trend in capacity loss and the acceleration of the capacity fade rate of the cell is observed. However, the other cells did not show significant increase on the degradation rate compared to cell NMC-017. As shown with the data tips of Fig. 10, the second life aging test is started at 3200 FECs (cell NMC-017), 1800 FECs (NMC-038), 1300 FECs (NMC-048), and 700 FECs (NMC-028). Among the four cells, the maximum resistance increase is found on the cell N028 at 300 FECs which was subjected to calendar aging during its first life. The resistance change for all the cells was not consistent and did not show a dominant change which normally is dependent on the electrochemical phenomena of the cells. Nevertheless, in addition to NMC-017, all the cells of NMC-038, NMC-048 and NMC-028 considered in the module level test shows noticeable capacity degradation.

VII. CONCLUSIONS AND FUTURE WORK

This paper presented the aging study of SLBs with the optimal sizing of the batteries for the dedicated stationary application accompanied by experimental study of real-life cycling profile.

The sizing approach used for the SLBs considers minimum size requirement to assure the storage system viability for the second life utilization. By using the proposed optimization algorithm and based on real power generation data taken from the PVGCS plant, the optimal rating of the SLBs is estimated. Besides the optimal sizing study of the SLBs, the cycling aging profile definition and synthesis was performed for the selected stationary application.

Based on the defined cycling test pattern, the most representative battery cells were selected and subjected to the second life battery aging tests. From the test result it is found that specific to the renewable power smoothing application, the SLBs provides relatively constant degradation rate of the capacity, showing that their technical performances are promising and therefore can be considered as viable solutions. Moreover, the aging result shows that, battery cells with around 80% of their FL-EoL criteria, can satisfy the second life stationary application with an average degradation rate of less than one percent for every 100 FECs. Based on capacity and internal resistance measurements found from prolonged cycling aging, a stopping criterion of 60% SoH limit is proposed for renewable power smoothing application considering the safety issues for aging of relatively high demanding stationary application. For both cell level and module level tests, the resistance change is not dominant interms of aging for these battery cells which makes it different from most of previous study results. In general, it is notable that the operating and testing conditions of the cells during their first life play a vital role on the SLBs performance and therefore these factors should be considered during the selection of potentially eligible SLBs for stationary application use. In the future, the research can further be investigated with consideration of pack level aging test in different stationary application perspective.

ACKNOWLEDGMENT

REFERENCES

[1] California air resources board, (2021), https://ww2.arb.ca.gov/our-work/programs/zero-emission-vehicle-program, (Date accessed: 07 September 2021).

[2] N. Cheeweewattanakoon, G. Kaur, N. Chawla, and O. Bruno, "Residential battery energy storage systems (BESS) modeling and effect on the smart grid from the classroom point of view," *ASEE Annu. Conf. Expo. Conf. Proc.*, 2014, doi: 10.18260/1-2--22978.

[3] H. A. Behabtu *et al.*, "A review of energy storage technologies' application potentials in renewable energy sources grid integration," *Sustain.*, vol. 12, no. 24, pp. 1–20, 2020, doi: 10.3390/su122410511.

[4] A. Hiendro, R. Kurnianto, M. Rajagukguk, Y. M. Simanjuntak, and Junaidi, "Techno-economic analysis of photovoltaic/wind hybrid system for onshore/remote area in Indonesia," *Energy*, vol. 59, pp. 652–657, 2013, doi: 10.1016/j.energy.2013.06.005.

[5] S. Saxena, C. Le Floch, J. MacDonald, and S. Moura, "Quantifying EV battery end-of-life through analysis of travel needs with vehicle powertrain models," *J. Power Sources*, vol. 282, pp. 265–276, May 2015.

[6] E. Cready, J. Lippert, J. Pihl, I. Weinstock, P. Symons, and R. G. Jungst, "Technical and economic feasibility of applying used EV batteries in stationary applications," 2003.

[7] B. Williams and T. Lipman, "Analysis of the Combined Vehicle - Use Value of Lithium-Ion Plug-In-Vehicle Propulsion Batteries. Task 3, Second Life Applications and Value of 'Traction' Lithium Batteries.," 2011.

[8] C. Curry, "New life for used EV batteries as stationary storage - Bloomberg New Energy Finance," Bloomberg Energy Finance. 2016.

[9] L. Ahmadi, A. Yip, M. Fowler, S. B. Young, and R. a. Fraser, "Environmental feasibility of re-use of electric vehicle batteries," *Sustain. Energy Technol. Assessments*, vol. 6, pp. 64–74, Jun. 2014.

[10] L. Ahmadi, M. Fowler, S. B. Young, R. a. Fraser, B. Gaffney, and S. B. Walker, "Energy efficiency of Li-ion battery packs re-used in stationary power applications," *Sustain. Energy Technol. Assessments*, vol. 8, pp. 9–17, Dec. 2014.

[11] J. Neubauer, K. Smith, E. Wood, A. Pesaran, J. Neubauer, K. Smith, E. Wood, and A. Pesaran, "Identifying and Overcoming Critical Barriers to Widespread Second Use of PEV Batteries Identifying and Overcoming Critical Barriers to Widespread Second Use of PEV Batteries," no. February, 2015.

[12] S. J. Tong, A. Same, M. a. Kootstra, and J. W. Park, "Off-grid photovoltaic vehicle charge using second life lithium batteries: An experimental and numerical investigation," *Appl. Energy*, vol. 104, pp. 740–750, Apr. 2013.

[13] A. A. Kebede et al., "A Techno-Economic Optimization and Performance Assessment of a 10 kWP Photovoltaic Grid-Connected System," Sustainability, vol. 12, no. 18, Sep. 2020, doi: 10.3390/su12187648.

[14] A. A. Kebede *et al.*, "Development of a lifetime model for large format nickel-manganese-cobalt oxide-based lithium-ion cell validated using a real-life profile," *J. Energy Storage*, vol. 50, p. 104289, 2022, doi: 10.1016/j.est.2022.104289.

[15] M. Gitizadeh and H. Fakharzadegan, ―Battery capacity determination with respect to optimized energy dispatch schedule in grid-connected photovoltaic (PV) systems,‖ *Energy*, vol. 65, pp. 665–674, Feb. 2014.

[16] H. Beltran, E. Perez, N. Aparicio, and P. Rodriguez, ―Daily Solar Energy Estimation for Minimizing Energy Storage Requirements in PV Power Plants,‖ *IEEE Transactions on Sustainable Energy*, vol. 4, no. 2. pp. 474–481, 2013.

[17] Y. Ru, J. Kleissl, and S. Martinez, ―Storage Size Determination for Grid-Connected Photovoltaic Systems,‖ *IEEE Transactions on Sustainable Energy*, vol. 4, no. 1. pp. 68–81, 2013.

[18] M. Z. Daud, A. Mohamed, and M. A. Hannan, "An improved control method of battery energy storage system for hourly dispatch of photovoltaic power sources," *Energy Convers. Manag.*, vol. 73, pp. 256–270, Sep. 2013.

[19]] S. Hashemi, J. stergaard, and G. Yang, "A Scenario-Based Approach for Energy Storage Capacity Determination in LV Grids With High PV Penetration," *IEEE Transactions on Smart Grid*, vol. 5, no. 3. pp. 1514–1522, 2014.

[20] M. S. Hosen *et al.*, "Twin-model framework development for a comprehensive battery lifetime prediction validated with a realistic driving profile," *Energy Sci. Eng.*, vol. 9, no. 11, pp. 2191–2201.